Journal of Nuclear Materials 386–388 (2009) 915–918

Contents lists available at ScienceDirect

Journal of Nuclear Materials

journal homepage: www.elsevier.com/locate/jnucmat

Modelling of radiation impact on ITER Beryllium wall

I.S. Landman *, G. Janeschitz

Forschungszentrum Karlsruhe, IHM, FUSION, P.O. Box 3640, 76021 Karlsruhe, Germany

A B S T R A C T

In the ITER H-Mode confinement regime, edge localized instabilities (ELMs) will perturb the discharge. Plasma lost after each ELM moves along magnetic field lines and impacts on divertor armour, causing plasma contamination by back propagating eroded carbon or tungsten. These impurities produce enhanced radiation flux distributed mainly over the beryllium main chamber wall. The simulation of the complicated processes involved are subject of the integrated tokamak code TOKES that is currently under development. This work describes the new TOKES model for radiation transport through confined plasma. Equations for level populations of the multi-fluid plasma species and the propagation of different kinds of radiation (resonance, recombination and bremsstrahlung photons) are implemented. First simulation results without account of resonance lines are presented.

1. Introduction

The operation of the future tokamak ITER will presumably be deteriorated by plasma contamination with wall species, which is determined by the inflow of eroded atoms through the separatrix and their ionization either in the scrape-off layer (SOL) or in the confinement region. A tungsten divertor would be preferable because the fraction of carbon-based material must be minimized due to the high tritium retention ability of carbon [1]. However, enhanced radiation losses of not fully ionized W-ions in the core may be dangerous as well for the discharge itself as for the beryllium main chamber wall.

For an integrated simulation of tokamak plasma equilibrium and surface processes with particular aim at the plasma contamination following outbreaks of edge localized mode (ELM), the code TOKES was recently designed [2]. Plasma fuelling, the magnetic field calculation, the Pfirsch–Schlüter plasma diffusion and thermal conductivity model, plasma impact onto the walls and the following influx of eroded neutrals from the walls have been implemented. Fig. 1 shows the TOKES implementation of the ITER vessel and the layers of confined plasma. The wall and the contours of the poloidal magnetic flux $w(r,z,t)$ obey toroidal symmetry and can have arbitrary poloidal shapes. The triangular grid coupled with the plasma layers allows calculations in the time t over the entire vessel.

The impurities cause enhanced radiation losses which can drive the operation of the tokamak towards increased plasma heating, and influence the electron temperature $T_e(w,t)$, in particular the separatrix temperature T_{eS}. In turn, T_{eS} determines the impurity influx by sputtering and thus T_{eS} becomes established self-consistently in the plasma wall interaction. After ITER ELMs, vaporization in vicinity of the separatrix strike point (SSP) can occur, which significantly increases the impurity influx and thus the radiation losses, especially with W-ions because they are not fully ionized in the quasi-neutral plasma and radiate in a wide recombination and resonance spectrum.

So far TOKES used only the radiation loss opacities of Ref. [3]. Here, we explain the implementation of a full radiation transport model, including resonance-, recombination- and bremsstrahlung radiation processes. The background formulas base on different theoretical sources (e.g. [4]) and are shortly listed in a unified manner in Section 2 to clarify implementation details of Section 3.

2. Radiation transport model

The free electrons are assumed to have the Maxwell's distribution $f_{eM}(\varepsilon_e)$ over the kinetic energy ε_e. The electron density N_e is the sum of population densities $N_{mzk}(w,t)$ over the energy states of bound electrons: $N_e = \Sigma z N_{mzk}$, with $m = 0,1,\ldots$ isotope index, $z = 0,1,\ldots$ charge state index and $k = 1,2,\ldots$ excited level index ($k = 0$ indicates the ground state). One part of $\partial N_{mzk}/\partial t$ is calculated using the plasma transport module. The ionization dynamics and radiation transport are described by separating them from the transport equations (splitting method), and $\partial N_{mzk}/\partial t$ in question is given by

$$\frac{\partial N_{mzk}}{\partial t} = S^{ed}_{mzk} + S^{ir}_{mzk} \tag{1}$$

The terms describe the excitation- and deexcitation transitions among the levels (S^{ed}) and the ionization and recombination (S^{ir}) of charge states, accounting for the impacts of both photons and free

* Corresponding author.
E-mail address: igor.landman@ihm.fzk.de (I.S. Landman).

0022-3115/$ - see front matter © 2009 Elsevier B.V. All rights reserved.
doi:10.1016/j.jnucmat.2008.12.330

electrons: $S^{ed} = P^{ed} + E^{ed}$ and $S^{ir} = P^{ir} + E^{ir}$. The description for E^{ed} and E^{ir} is based on the excitation- $\sigma^{Ee}(\varepsilon_e)$ and ionization $\sigma^{Ei}(\varepsilon_e)$ cross-sections. Given the cross-sections, TOKES calculates the process rates $r(T_e) = <\sigma^{Ei} v_e>$ with $v_e = (2\varepsilon_e/m_e)^{1/2}$ the electron velocity.

In a tokamak plasma the assumption of a Planck radiation intensity $I_P(\varepsilon, T_e)$ is not justified and generally $I_p(w, \varepsilon, \mathbf{s})$ depends both on the photon energy ε and the direction vector $\mathbf{s}$. The photon absorption by photoionization and photoexcitation (and the inverse bremsstrahlung) is described in terms of the emission coefficient β and the absorption coefficient κ' (κ' includes both spontaneous and induced radiation). Introducing a coordinate s along the beam, the Buger's law is assumed: $dI_p/ds = \beta(s) - \kappa'(s) I_p$.

The terms S^{ed} and S^{ir} of Eq. (1) follow as (m is omitted):

$$S_k^{ed} = \sum_{k'=0}^{k-1} \left(v_{k'k}^{e} N_{k'} - v_{k'k}^{d} N_k\right) + \sum_{k'=k+1}^{K} \left(v_{kk'}^{d} N_{k'} - v_{kk'}^{e} N_k\right) \tag{2}$$

$$S_{zk}^{ir} = v_{zk}^{r} N_{z+1,0} - v_{zk}^{i} N_{zk} + \delta_{k0} \sum_{k'=0}^{K_{z-1}} \left(v_{z-1,k'}^{i} N_{z-1,k'} - v_{z-1,k'}^{r} N_{z0}\right) \tag{3}$$

The frequencies v contain both electron- and photon impact contributions. For instance the excitation frequency for a resonance transition $l = (kk')$ is the sum $v_{kk'}^{e} = v_{kk'}^{Ee} + v_{kk'}^{Pe}$. Only the recombination/ionization transitions between the levels E_{zk} and the ground state $E_{z+1,0}$ are accounted for, $\delta_{k0} = 1$ at $k = 0$, otherwise $\delta_{k0} = 0$. Some maximum level K is set.

For the electron impacts we have $v_l^{Ee} = N_e r_l^{Ee}$ and $v_{zk}^{Ei} = N_e r_{zk}^{Ei}$, with r the process rate. For the inverse frequencies v_l^{Ed} and v_{zk}^{Er} the detailed balance principle (the Klein–Rosseland formula) is used, which results in the Boltzmann's relation:

$$v_l^{Ed} = v_l^{Ee} (g_k/g_{k'}) \exp(\Delta E_l/T_e) \tag{4}$$

The g_k are level's statistical weights and $\Delta E_l = E_{k'} - E_k > 0$ the transition energy.

The balance relation between v_{zk}^{Ei} and v_{zk}^{Er} is obtained using Eq. (3) at thermodynamic equilibrium with omitted radiation contributions: $S_{zk}^{ir} = E_{zk}^{ir} = 0$ and the Saha formula, which results in the relation:

$$v_{zk}^{Er} = v_{zk}^{Ei} (g_{zk}/g_{z+1,0}) \left(N_e/N^S\right) \exp(I_{zk}/T_e) \tag{5}$$

Here $I_{zk} = E_{z+1,0} - E_{zk}$ is the ionization energy, $N^S = \frac{1}{4}\pi^{-3/2} \cdot (T_e/Ry)^{3/2}/(r_B)^3$ the Saha density, Ry the Rydberg constant, and r_B the Bohr radius.

For resonance transitions (radiation lines) the expressions for the resonance opacities read:

$$\beta_l = (4\pi)^{-1} A_l L_l(\varepsilon) \Delta E_l N_{k'} \tag{6}$$

$$\kappa_l' = A_l \left(\frac{\pi c \hbar}{\Delta E_l}\right)^2 \hbar L_l(\varepsilon) \left(\frac{g_{k'}}{g_k} N_k - N_{k'}\right) \tag{7}$$

Here A_l [s^{-1}] is the Einstein coefficient and $L_l(\varepsilon)$ the line shape. The excitation frequency reads:

$$v_l^{Pe} = A_l \frac{\pi^2 c^2 \hbar^3}{E_l^3} \frac{g_{k'}}{g_k} \int L_l(\varepsilon) I(\varepsilon, \mathbf{s}) d\varepsilon d\mathbf{s} \tag{8}$$

Then the deexcitation frequency follows as $v_l^{Pd} = A_l + (g_k/g_{k'}) v_l^{Pe}$.

For the recombination radiation, the cross-sections of photoionization and spontaneous recombination are related according to the Miln formula, which results in

$$v_{zk}^{Pi} = \int_{I_{zk}}^{\infty} \sigma_{zk}^{Pi}(\varepsilon) \frac{d\varepsilon}{\varepsilon} \int_{4\pi} I(\varepsilon, \mathbf{s}) d\mathbf{s} \tag{9}$$

Using the equality $\varepsilon = I_{zk} + \varepsilon_e$, v_{zk}^{Pr}, β_{zk} and κ_{zk}' are also expressed in terms of σ^{Pi}. For instance, the absorption coefficient for recombination radiation is given by

$$\kappa_{zk}' = \sigma_{zk}^{Pi}(\varepsilon) \left(N_{zk} - \frac{g_{zk}}{g_{z+1,0}} \frac{N_e N_{z+1,0}}{N^S} \exp\left(\frac{I_{zk} - \varepsilon}{T_e}\right)\right) \tag{10}$$

Finally, the Maxwell's distribution of free electrons provides the validity of the Kirchhoff's law $\kappa_b'(\varepsilon) = \beta_b(\varepsilon)/I_P(\varepsilon)$ for the bremsstrahlung opacities $\beta_b(\varepsilon)$ and $\kappa_b'(\varepsilon)$.

3. Implementation of radiation transport

A database for basic atomic parameters such as level energies, Einstein coefficients, statistical weights, ionization potentials, excitation rates and ionization cross-sections, is implemented. Only necessary populations for N_{mzk} are processed with ranges $z_{1m} \leqslant z \leqslant z_{2m}$ for ion charges and $0 \leqslant k \leqslant K_{mz}$ that vary over the plasma layers being changed at discrete moments t_n; off the ranges N_{mzk} are zeroed keeping conservation of particles and energy. Numerical integration of Eq. (1) is done for each layer using the implicit finite-difference scheme of type

$$\mathbf{N}(t_n) - \mathbf{N}(t_{n-1}) = \hat{v}(t_{n-1}) \mathbf{N}_n \Delta t_n \tag{11}$$

Here $\mathbf{N}$ is the vector of N_{mzk} and $\hat{v}$ the frequency matrix. A stable algorithm for the effective solution of Eq. (11) with arbitrary time steps $\Delta t_n = t_n - t_{n-1} > 0$ is available.

A Monte-Carlo technique for the propagation of neutrals as 'representative rays' through the triangular meshes is described in detail in [2]. However, for photons it accounts only for the absorption contribution, and the emission term is split off. The radiation rays are directed randomly, with isotropic distribution on $\mathbf{s}$. One ray starts from a random point $\mathbf{r}_0$ of a plasma layer uniformly distributed over its volume V. There is minimum $\varepsilon_{\min}$ and maximum $\varepsilon_{\max}$ of the allowed photon energy, e.g. $\varepsilon_{\min} = 0.3 T_{\min}$ and $\varepsilon_{\max} = 30 T_{\max}$, with $T_{\min}$ and $T_{\max}$ the extreme values of T_e over the plasma.

The integration is performed as follows. The first step is the accumulation of the emitted radiation in special numerical stores of the layers. During a time step Δt the stored energy is $Q = 4\pi\beta(\varepsilon) V \Delta\varepsilon \Delta t$ with ε and $\Delta\varepsilon$ some values specified below; $\beta(\varepsilon)$ depends also on N_{mzk} and T_e and thus stays constant over the layer.

The second step is the propagation of the stored photons. For reabsorption of a radiation portion $Q > 0$ in the layers the absorption part is approximated as

$$Q(s_i) - Q(s_{i-1}) = \Delta Q_i = -\kappa'_i Q(s_j) \delta s_i \tag{12}$$

The coordinates s_i ($i > 0$) designate sequential ray crossings of layer boundaries, $\delta s_i = s_i - s_{i-1} > 0$ and $s_0 = 0$ the starting point $\mathbf{r}_0$. The total absorption coefficient κ_i' corresponds to the layer (s_{i-1}, s_i). For numerical stability, if κ_i' is positive then $j = i$, otherwise $j = i - 1$.

In every layer each available resonance transition (mzl) is supplied with one own store, each level (mzk) gets also one, and the bremsstrahlung gets several (e.g. $J = 16$) stores. The bremsstrahlung is accumulated for some photon energy intervals $\Delta\varepsilon_j = \varepsilon_j - \varepsilon_{j-1}$ determined by the boundary energies ε_j of the stores. The line radiation is stored assuming the resonance photon energy: $\varepsilon = E_{mzl}$, and $\Delta\varepsilon = \Delta\varepsilon_{mzl}$ a line width. The recombination radiation is stored assuming some $\varepsilon = \varepsilon_{mzk}$ and $\Delta\varepsilon_{mzk}$ outgoing from an averaging over $\sigma_{zk}^{Pr}(\varepsilon)$.

At every time step each store is cleared by emitting the accumulated energy. The emitted ray has a random energy value ε_r, whereby on the average ε_r equals ε. At first the resonance- and recombination photons are emitted, and secondly the bremsstrahlung ones, with appropriate distributions of ε_r corresponding to either the line shapes $L(\varepsilon)$ or the cross-sections $\sigma^{Pi}(\varepsilon)$. The carriers

of $L(\varepsilon)$ and $\sigma^{Pi}(\varepsilon)$ are reasonably cut: e.g. $|\varepsilon - E_l| \leqslant 10\Delta\varepsilon_l$ and $I_{zk} \leqslant \varepsilon \leqslant 10I_{zk}$. The emission process is repeated until all stores are completely emptied.

The amount of reabsorbed photons $n_i = \Delta Q_i/\varepsilon_r$ of a resonance radiation store allows to obtain the photoexcitation frequency $\nu_l^{Pe} = n_i/(V\Delta t)$, and similarly ν_{zk}^{Pi}.

4. First simulation results on radiation transport

Because the TOKES database for resonance transitions is up to now too poor for adequate simulations of line contributions, at present only the steady state regime is simulated for the radiation load onto the whole wall surface, but not the resonance radiation and excited levels. Nevertheless, such simplified demonstration is reasonable due to the fact that the minimum temperature over the confined plasma region is about 1.5 keV in current simulations

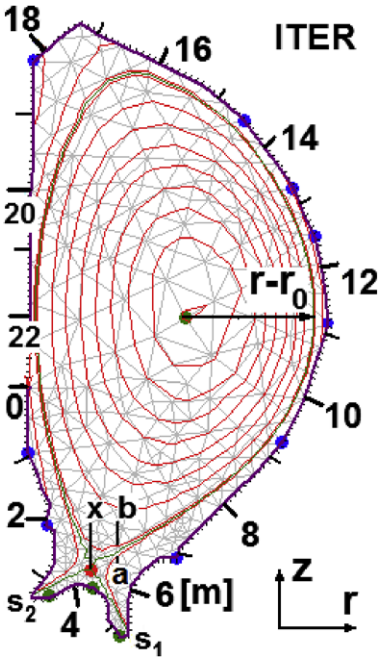

Fig. 1. The ITER layout and the wall coordinate X, with the circles marking the extremes of the magnetic flux w.

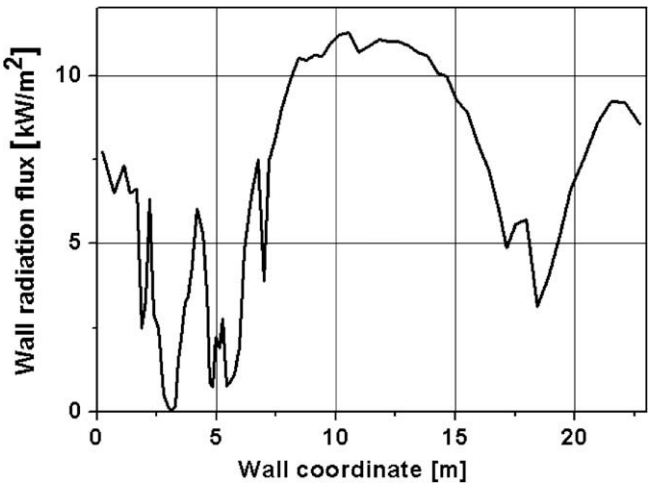

Fig. 2. Wall radiation flux in steady ITER discharge.

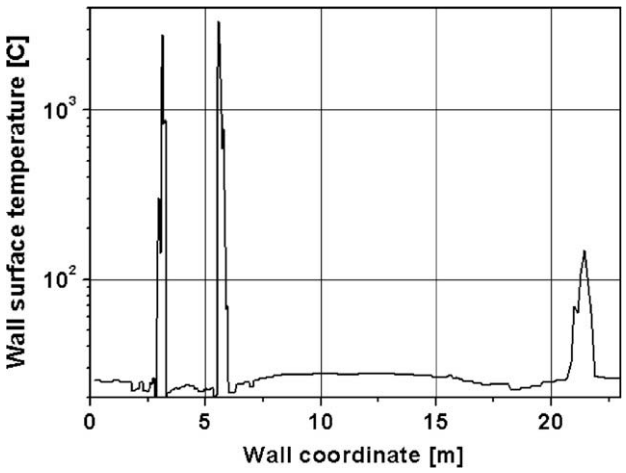

Fig. 3. Wall surface temperature in steady state ITER discharge. The three temperature peaks are due to direct plasma impact.

[5]. Thus all involved species but tungsten impurity ions are fully ionized and bremsstrahlung becomes the most important kind of radiation.

For a Be–C–W wall at discharge time $t = 150$ s, Fig. 2 shows the radiation load distribution as a function of the wall coordinate of Fig. 1, and Fig. 3 the profile of the surface temperature. The simulation was carried out with 5 cm wall thickness, 20 °C outer temperature and the bulk thermal conductivities 70 (Be), 200 (CFC) and 90 (W) W/mK. The radiation load is obtained to be rather small (11 kW/m^2) and thus a rather small temperature rise follows (about 10°). Simultaneously the temperature in vicinity of the separatrix strike points (designated with s_1 and s_2 on Fig. 1) in the divertor reached a very high value of 3150 K (which is below the excessive vaporization point). In this regime the plasma heat outflow reaches 90 MW and the radiation losses 6.6 MW, which does not exceed significantly the previous result 5 MW [5] obtained using the data [3]. The losses are balanced by the fusion power 74 MW of α-particles and the beam power 22.6 MW.

5. Conclusions

A full radiation transport model that includes both level populations and a Monte-Carlo technique for photon ray propagation allowing for plasma reabsorption has been implemented. The recombination- and bremsstrahlung photons are simulated with representative rays that are naturally coupled with the confined plasma. By this, TOKES acquired major features necessary for two-dimensional integrated tokamak modelling.

However, the code cannot yet perform complete radiation transport calculations, because appropriate resonance transition data are not available, and at this stage only steady state simulations are justified. The steady state wall heating caused by radiation is obtained to be negligible in comparison with that of direct plasma impact.

The most urgent step for improvement of the radiation transport model is to include the data for atomic levels and the resonance transitions. This would allow expanding the applicability of TOKES for ELMy H-Mode simulations and comparing modelling results with experiments at existing big tokamaks. In particular, in the steady state, plasma detachment can occur with low pre-surface temperature, which implies a significant role of line radiation there. However, for simulating the detachment the implementation of the scrape-off layer will also become necessary in the integrated code.

Acknowledgements

This work, supported by the European Communities under the contract EFDA/05-1305 of Association between EURATOM and Forschungszentrum Karlsruhe, was carried out within the framework of the European Fusion Development Agreement. The views and opinions expressed herein do not necessarily reflect those of the European Commission.

References

[1] M. Shimada et al., Nucl. Fus. 47 (2007) S12.
[2] I.S. Landman, G. Janeschitz, J. Nucl. Mater. 363–365 (2007) 1061.
[3] D.E. Post et al., Atom. Data Nucl. Data Tables 20 (1977) 397.
[4] H.R. Griem, Radiation processes in plasmas, in: M.N. Rosenbluth, R.Z. Sagdeev (Eds.), Handbook of Plasma Physics, vol. 1, 1983, p. 73.
[5] I.S. Landman, G. Janeschitz, Fus. Eng. Des. 83 (2008) 1797.